

Intercept of Frequency Agility Signal using Coding Nyquist Folding Receiver

KEYU LONG

School of Electronic Engineering
University of Electronic Science and Technology of China
No. 2006, Xiyuan Avenue, West Hi-Tech Zone, Chengdu
CHINA
longkeyu_2008@163.com

Abstract: - The parameter estimation of the frequency agility (FA) signal using the coding Nyquist folding receiver (CNYFR) is presented. The estimation algorithm adopting linear frequency modulation (LFM) as the local analogue modulation is derived. The Nyquist zone is estimated by the pseudo Wigner-Ville distribution (PWVD) and the hopping frequencies are calculated by the maximum likelihood (ML) method. Simulations show that CNYFR with analogue modulation of LFM has better performance than the sinusoidal frequency modulation (SFM) one, and the parameter estimation accuracy is acceptable when the SNR is above 0dB.

Key-Words: - Frequency agility signal; Nyquist folding receiver; coding; linear frequency modulation (LFM).

1 Introduction

The frequency agility (FA) signal, also known as the frequency hopping (FH) signal, has been widely applied in radar, communication, sonar and other fields because of its good performance in low possibility of intercept and anti-interference. In the field of radar, FA has always been a research focus. Bellegarda studied multiple access FH signals using a synthesis tool of the hit array in the context of coherent active radar [1]. Morrison proposed an approach which allows the frequency spectrum to be greatly under-sampled to provide a greater effective bandwidth for a stepped frequency continuous wave (SF-CW) synthetic aperture radar (SAR) [2]. Becker studied passive localization of FA radars for angle and frequency measurements [3]. Rogers presented analytical techniques for evaluating the performance of FH radars based on the autocorrelation properties of the frequency selection process [4]. Lellouch investigated an agile orthogonal frequency division multiple (OFDM) waveform to solve the problem of Doppler frequency shift in FA [5].

The bandwidth of a FA radar signal could be greater than 10GHz. For the intercept receiver of the FA signal, the main question is how to intercept such a wide bandwidth under the condition of low sampling rate less than 3Giga sample per second (GSPS). Fortunately, the FA signal could be regarded as a kind of sparse signals, and could be processed by the recent powerful concept denoted as compressed sensing (CS). Under CS, we may intercept the radar signals with low sampling rate.

The concept of CS was proposed by Candes and Donoho [6-7], et al in 2006. From then on, many scholars studied the application of CS in various aspects. Herman studied a high-resolution radar via CS [8]. Ma used CS for surface characterization and metrology [9]. Potter applied CS in radar imaging [10]. Provost studied the application of CS for photo-acoustic tomography [11]. Flandrin discussed the connection between CS and time frequency distribution, and showed that improved representations can be obtained with the cost of computational complexity [12]. Now CS has been applied to a variety fields such as receiver and camera.

In the receiver side, some scholars have proposed different structures. Tropp and Laska developed an architecture called the random demodulator, which consists of a pseudorandom number generator, a mixer, an accumulator (or a low pass filter) and a low rate analog-to-digital converter (ADC). First, they mixed the input signal with a high-rate pseudo noise sequence. Then, the output signal passes through a filter with a narrow passband and a few samples with a relatively low rate compared to the Nyquist rate are acquired. The system can be used to perform the spectrum sensing, geophysical imaging as well as radar and sonar imaging. The major advantage of the random demodulator is that it avoids a high-rate ADC, and expands the CS theory to analog signals. Also, it is robust against noise. However, some engineering issues should be considered such as the speed of the mixer and the

impulse response of the filter [13-14]. Romberg proposed another structure called random convolution. It circularly convolves the input signal with a random pulse and then subsamples the output signal. Since the system is universal and allows fast computations, it is perfect to be a theoretical sensing strategy. Some applications include radar imaging and Fourier optics. The random convolution system is simpler and more efficient than other random acquisition techniques. Further, the system is suited to a wide range of compressed signals. However, the realization of random pulse is a challenging problem. For instance, whether different shifts of the pulse are orthogonal is still a problem [15-16].

In the application of camera, Takhar developed a new camera architecture called compressive imaging camera, which uses a digital micro mirror array to acquire linear projections of an image onto pseudorandom binary patterns. The most exciting feature of the system is that it can be adapted to image at wavelengths with conventional charge-coupled device (CCD) and complementary metal oxide semiconductor (CMOS) imagers, and it has good features including simplicity, universality, robustness, and scalability. However, some problems still exist as follows; for example, more other measurement bases can be implemented, and higher-quality reconstruction of images needs further studies. Besides, a more complex photon sensing element can be used to colour, multispectral, and hyper spectral imaging [17].

Driven by the idea of CS, Fudge proposed the Nyquist Folding Receiver (NYFR) [18]. This type of receiver overcomes the disadvantages of the traditional sub-sampling technique, only aiming at a particular Nyquist sampling, and avoids frequency sweep. The key of the NYFR is that the Nyquist zone could be mapped to a parameter of the local analogue modulated signal on the received signals, and then we can sample the received signals which contain the additional Nyquist zone information by a low sampling rate. By changing the bandwidth of local analogue modulation and the channel number, we can achieve the whole probability interception of a wideband or ultra-wideband signal in one channel without using frequency sweep. However, the structure of NYFR is easily affected by noise at the zero crossing rising (ZCR) time when controlling the radio frequency (RF) sample clock of shape pulse using a full analogue structure for wideband modulation. Besides, the structure of single channel limits interception bandwidth mostly and the implementation of sinusoidal frequency modulation (SFM) as a local analogue modulation is difficult.

This paper presents an improved structure marked as coding NYFR (CNYFR), also called dual channel NYFR (DCNYFR) to realize the interception of the FA signal, and shows the algorithm using pseudo Wigner-Ville distribution (PWVD) for the estimation of the Nyquist zone. Moreover, since linear frequency modulation (LFM) is easier to be generated, we adopt LFM as the local analogue modulation instead of SFM.

The rest of the paper is organized as follows. Section 2 analyses the structure for CNYFR in details, and gives the advantages of dual-channel. Section 3 describes the estimation of Nyquist zone. Section 4 provides simulations. Finally, section 5 concludes the paper.

2 Coding Nyquist Folding Receiver

With continued improvements in digital signal processing (DSP) technology, the ADC is becoming one of the bottlenecks in a variety of signal applications ranging from radar to communications, where the information is processed within extremely wide RF bandwidths. Since the environment of signal applications is generally sparse, it is feasible to reduce the sample rate. Fudge considered the information sampling of these sparse signals and presented a practical receiving structure called NYFR which can be applied to the direct processing of high RF signals.

2.1 Structure for CNYFR

We pay attention to the NYFR which is an analog-to-information receiver architecture. The key technique is that it folds the multiple original signal component frequencies into a narrow bandwidth prior to ADC. In this case, the sample rate of ADC can be reduced obviously. Base on the architecture of the NYFR, we can make some advances and propose this CNYFR.

The structure of the CNYFR is shown in Fig.1. Assume that the input signal is FA, and the agile range is from several hundreds of MHz to 20GHz. Besides, we assume the input analog signal has been pre-processed into a complex signal. Firstly, the input signal is filtered by a ultra wideband (UWB) low-pass filter (LPF_1) whose passband is up to 20GHz to remove the out-of-band noise to get the complex signal $x(t)$. Then, $x(t)$ is multiplied by $p_i(t)$, $i=1,2$, to obtain the modulated signal $r_i(t) = x(t)p_i(t)$, then $r_i(t)$ is filtered by the second complex low-pass filter (LPF_2) with the passband $[-f_s/2, f_s/2]$ to get the signal $s_i(t)$, where f_s is

the sampling rate for ADC. Finally, sample signal $s_i(t)$ by the rate of f_s to obtain $s_i(n)$. Then, $s_i(n)$ will be sent to DSP for the estimation of the Nyquist zone. In this paper, different from the NYFR, $p_i(t)$ is generated by the direct digital synthesizer (DDS)

and digital analog converter (DAC), where DDS is constituted of f_s , the phase $\theta(n)$ and the initial phase φ_0 .

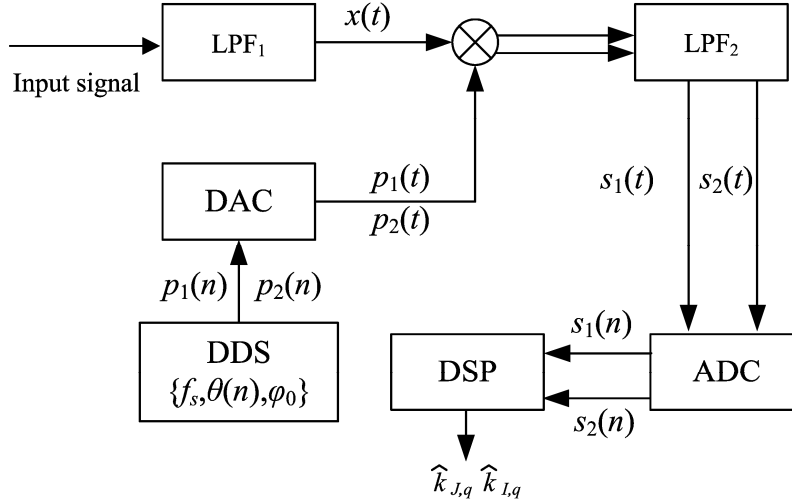


Fig.1. The structure of CNYFR

For $p_1(t)$ and $p_2(t)$, we draw on the idea of code-division multiple access (CDMA). In CDMA communication system, the signal which the users adopt to transmit different information is not discriminated from each other by different frequencies or time slots, but by their own coding sequences or different waveforms of signals. Similarly, in the NYFR, we introduce the coding mechanism and generate the UWB analogue modulation oscillators $p_1(t)$ and $p_2(t)$ to stand for different Nyquist zones of the whole frequency band we are interested in. First of all, we divide the interception bandwidth B_I into N sub-bands. The bandwidth of each sub-band is fixed to $K_1 f_s$, where K_1 is the factor of coding. Then, on the one hand, the bandwidth for $p_1(t)$ increases exponentially by kB_θ in each sub-band where $k \in \{1, 2, \dots, K_1\}$, and B_θ is the bandwidth of $\theta(t)$, where $\theta(t)$ is the phase modulation function, such as a sinusoidal function, a polynomial function, etc. Meanwhile, the waveforms are the same among the sub-bands. In this case, the $p_1(t)$ can be given by

$$p_1(t) = 1 + \sum_{n=1}^N \sum_{k=1}^{K_1} e^{j\{k(2\pi f_s t + \varphi_0) + [k - (n-1)K_1]\theta(t)\}} \quad (1)$$

where φ_0 is the initial phase and $n \in \{1, 2, \dots, N\}$.

On the other hand, the bandwidth for $p_2(t)$ is fixed in each sub-band and increases exponentially by nB_θ among the sub-bands. So $p_2(t)$ can be given by

$$p_2(t) = 1 + \sum_{n=1}^N \sum_{k=1}^{K_1} e^{j[k(2\pi f_s t + \varphi_0) + n\theta(t)]} \quad (2)$$

2.2 Theoretical analysis

Considering $x(t)$ is frequency agile, which is denoted as

$$x(t) = \sum_{q=0}^{Q-1} e^{j(2\pi f_q t + \varphi_q)} \mu(t - qT_r) \quad (3)$$

where

$$\mu(t) = \begin{cases} 1, & 0 \leq t < T_p \\ 0, & \text{otherwise} \end{cases};$$

T_p width of sub-pulse;

T_r pulse repetition interval (PRI);

$T_r > T_p$;

f_q agile frequency;

φ_q initial phase for the q th sub-pulse;

Q the number of components.

The NYFR presented by Fudge used the ZCR voltage of SFM to control the shaping pulse to get the UWB analogue modulation $p(t)$. While, the key of the NYFR is to move the local wideband signals, such as FA, with different Nyquist zones into the baseband. As long as the analogue modulation has different band information in each corresponding Nyquist zone, we can get the same result in the NYFR. Therefore, the analogue modulation could be simply rewritten as equation (1) and equation (2).

According to equation (1) and equation (2), the maximum interception bandwidth can be expressed as

$$B_l = (NK_1 + 1/2)f_s \quad (4)$$

After being mixed and filtered by LPF₂, the outputs should be

$$s_1(t) = \sum_{q=0}^{Q-1} e^{j[2\pi(f_q - f_s k_{H,q})t + \varphi_q - k_{H,q}\varphi_0 - k_{l,q}\theta(t)]} \mu(t - qT_r) \quad (5)$$

$$s_2(t) = \sum_{q=0}^{Q-1} e^{j[2\pi(f_q - f_s k_{H,q})t + \varphi_q - k_{H,q}\varphi_0 - k_{J,q}\theta(t)]} \mu(t - qT_r) \quad (6)$$

where

$$k_{l,q} = \text{round}[(f_q - k_{J,q}K_1 f_s) / f_s];$$

$$k_{J,q} = \lceil f_q / K_1 f_s \rceil;$$

$\lceil \cdot \rceil$ stands for round down;

$$k_{J,q} \in [0 \quad N-1];$$

$$k_{l,q} \in [1 \quad K_1].$$

$$k_{H,q} = k_{H,q} - (n_{H,q} - 1)K_1 \quad (7)$$

$$k_{J,q} = n_{H,q} - 1 \quad (8)$$

Substituting equation (8) into equation (7), we get

$$k_{H,q} = k_{l,q} + k_{J,q}K_1 \quad (9)$$

Sample $s_1(t)$ and $s_2(t)$ then

$$s_1(n) = \sum_{q=0}^{Q-1} e^{j[2\pi(f_q - f_s k_{H,q})nT_s + \varphi_q - k_{H,q}\varphi_0 - k_{l,q}\theta(nT_s)]} \mu(nT_s - qT_r) \quad (10)$$

$$s_2(n) = \sum_{q=0}^{Q-1} e^{j[2\pi(f_q - f_s k_{H,q})nT_s + \varphi_q - k_{H,q}\varphi_0 - k_{J,q}\theta(nT_s)]} \mu(nT_s - qT_r) \quad (11)$$

where $T_s = 1/f_s$ is the sampling interval.

From equation (10), we know that the q th sub-pulse of the output $s_1(n)$ is a wideband signal whose center frequency, bandwidth and initial phase are $f_q - f_s k_{H,q}$, $B_{s1} = k_{l,q}B_\theta$ and $\varphi_q - k_{H,q}\varphi_0$, respectively. The q th sub-pulse of the output $s_2(n)$ is also a wideband signal which has the same centre frequency and initial phase but different bandwidth $B_{s2} = k_{J,q}B_\theta$.

2.3 The choice of the local analogue modulation

In this paper, we chose frequency modulation (FM) as the local analogue modulation. Like the

amplitude modulation (AM), FM is well known as a broadcast signal format for communication. In particular, the LFM signal is a kind of FM signal whose instantaneous frequency (IF) is modulated by a linear signal. Because of low probability of intercept, it is one of the most important signals in radar field, which has high range resolution, inhibits leakage and near field interference. Due to its good pulse compression characteristic, many high resolution radars such as SARs use this kind of FM waveform. It is a mature technology to generate the waveform; therefore, we are more inclined to choose LFM than SFM as the local analogue modulation.

2.4 The advantage of Dual-channel

The signals $s_1(t)$ and $s_2(t)$ are just in one Nyquist zone namely the baseband $[-f_s/2 \quad f_s/2]$. According to the Nyquist sampling theorem, the condition of sampling without aliasing is

$$k_{l,q}B_\theta \leq K_1B_\theta$$

$$= (B_l / f_s - 1/2)B_\theta / N \quad (12)$$

$$\leq f_s$$

Suppose that we use SFM function $\theta(t)$, i.e.,

$$\theta(t) = t_e \sin(2\pi f_f t) \quad (13)$$

The instantaneous frequency of equation (13) is $f = t_e f_f \cos(2\pi f_f t)$, therefore $B_\theta = 2t_e f_f$, where $t_e = \Delta f / f_f$ is the factor of frequency modulation, Δf the frequency drift and f_f the frequency of the modulation signal.

Equation (12) could be rewritten as

$$t_e \leq \frac{f_s^2 N}{2B_l f_f - f_s f_f} \quad (14)$$

Generally, for SFM, t_e is one of the most important parameters we need to design. Compared with the single channel method, the dual-channel can realize wider B_l with the same parameters of SFM. When $f_s \ll B_l$ and $t_e \leq f_s^2 N / 2B_l f_f$, B_l can be widened N times.

We can recover the signal without distortion when equation (12) is satisfied. For electronic reconnaissance, when the interception frequency range is 21GHz, the sampling rate is 2GHz and $K_1 = 5$, we get $N = 2$ from equation (4), then $B_\theta \leq 400$ MHz.

$p_1(t)$ and $p_2(t)$ using SFM and LFM are shown in Fig.2 and Fig.3, respectively.

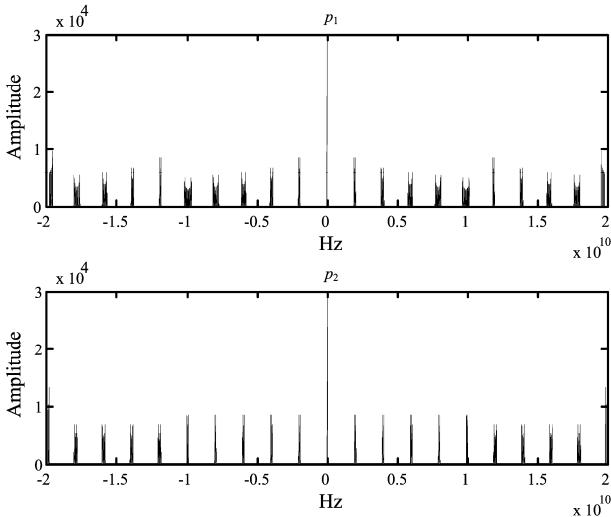


Fig.2. $p_1(t)$ and $p_2(t)$ using SFM

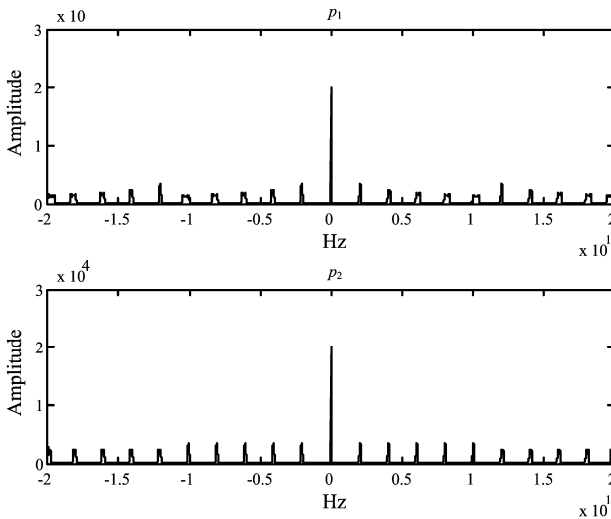


Fig.3. $p_1(t)$ and $p_2(t)$ using LFM

2.5 The advantage of the CNYFR

The proposed CNYFR has developments over the NYFR in the following aspects:

The structure of the NYFR used convolution of a Dirac sequence with the pulse template to generate the local analogue modulation, therefore, it results in too complex theoretical analysis and there are lots of approximate equivalent; while, the derivation of the CNYFR for local analogue modulation showed in (1) and (2) are easy to understand, and avoid approximate equivalent.

Moreover, the structure of the NYFR is easily affected by noise at the time of ZCR when controlling the RF sample clock of pulse template using a full analogue structure for wideband modulation. Differing from the NYFR, the pulse train $p_i(t)$ is generated by the DDS and digital analog converter DAC, where DDS is constituted of f_s , the phase $\theta(n)$ and the initial phase φ_0 . The

$p_i(t)$ and DSP of the CNYFR are synchronous, and we can estimate the initial phase of the received signal easily.

3. The estimation of the Nyquist zone

Before estimating the Nyquist zone, we assume that the signal has been detected with a relevant algorithm. After the detection, we could estimate the parameters of the Nyquist zone.

As mentioned above, the outputs of $s_1(n)$ and $s_2(n)$ are wideband signals where the centre frequency, bandwidth and initial phase are $f_q - f_s k_{H,q}$, $k_{L,q} B_\theta$ and $\varphi_q - k_{H,q} \varphi_0$ for $s_1(n)$; $f_q - f_s k_{H,q}$, $k_{J,q} B_\theta$ and $\varphi_q - k_{H,q} \varphi_0$ for $s_2(n)$, respectively. We could estimate the Nyquist zone $k_{L,q}$ using the time-frequency distribution (TFD) such as PWVD by dividing the bandwidth B_{s1} corresponding to the amplitude of the ridge of TFD and the bandwidth B_θ . In the same way, we could estimate the Nyquist zone $k_{J,q}$. Then, we use equation (9) to estimate the final Nyquist zone $k_{H,q}$.

Because the FA signal has multiple components, the problem of cross-terms exists. In order to get accurate parameter estimation, it is necessary to reduce the effects of cross-terms. Therefore, we adopt the TFD namely PWVD. PWVD is derived from the WVD. WVD is based on the stationary property of quadratic signal form. As the quadratic form of $s_1(n)$ is not always stationary, we should use PWVD.

The definition of PWVD is as follows:

$$PWD_s(t, f) = \int_{-\infty}^{+\infty} s(t + \tau/2) s^*(t - \tau/2) h(\tau) e^{-j2\pi f \tau} d\tau \quad (15)$$

where $h(\tau)$ is the window function.

In order to validate the effectiveness of the method, we set the polynomial function as $\theta(t)$, and

$$\theta(t) = \pi k t^2 \quad (16)$$

where k is the slope of modulation.

We assume that $h(\tau)$ is a Gaussian window

$$h(\tau) = e^{-\alpha \tau^2} \quad (17)$$

Under this condition, equation (5) or equation (6) is a LFM. We just rewrite them to the unified expression

$$s(t) = e^{j2\pi(f_0 t + 0.5 k t^2 + \varphi_i)} \quad (18)$$

where φ_i is the initial phase.

The product signal is

$$\begin{aligned}
 & s(t + \tau / 2) s^*(t - \tau / 2) \\
 & = e^{j2\pi[f_0(t+\tau/2)+1/2k(t+\tau/2)^2+\phi_0]} \cdot \\
 & e^{-j2\pi[f_0(t-\tau/2)+1/2k(t-\tau/2)^2+\phi_0]} \\
 & = e^{j2\pi(f_0+kt)\tau}
 \end{aligned} \tag{19}$$

Then inserting equation (19) into equation (15), the PWVD of LFM is as follows:

$$\begin{aligned}
 PWD_s(t, f) & = \\
 & \int_{-\infty}^{+\infty} s(t + \tau / 2) s^*(t - \tau / 2) h(\tau) e^{-j2\pi f \tau} d\tau \\
 & = \int_{-\infty}^{+\infty} e^{j2\pi(f_0+kt)\tau} h(\tau) e^{-j2\pi f \tau} d\tau
 \end{aligned} \tag{20}$$

According to the convolution property of the Fourier transform, we know that the product in time domain means convolution in frequency domain. Therefore, equation (20) is equal to

$$PWD_s(t, f) = \delta[f - (f_0 + kt)] \otimes H(f) \tag{21}$$

where the mark \otimes denotes one dimension convolution at frequency f . Here we use

$$\begin{aligned}
 & \int_{-\infty}^{+\infty} e^{j2\pi(f_0+kt)\tau} e^{-j2\pi f \tau} d\tau \\
 & = \int_{-\infty}^{+\infty} e^{j2\pi(f_0+kt-f)\tau} d\tau \\
 & = \delta[f - (f_0 + kt)]
 \end{aligned} \tag{22}$$

and

$$H(f) = \pi^{1/2} \alpha^{-1/2} e^{-(\pi f)^2 / \alpha} \tag{23}$$

is the Fourier transform of $h(\tau)$, which is monotonously decreasing, and we can get the maximum of $H(f)$ at $f = 0$.

Then by equation (21) and equation (23), we can get

$$\begin{aligned}
 PWD_s(t, f) & = H(f - (f_0 + kt)) \\
 & = \pi^{1/2} \alpha^{-1/2} e^{-(\pi[f - (f_0 + kt)])^2 / \alpha}
 \end{aligned} \tag{24}$$

The ridge of PWVD contains important information about the characteristics of the signal. We put forward an algorithm to extract the ridge. The idea is to search for the maximum of $PWD_s(t, f)$ along f . Thus, the ridge of $PWD_s(t, f)$ is given by

$$r(t) = \arg \max_f \{ PWD_s(t, f) \} \tag{25}$$

Based on analysis above, we know that equation (24) gets the maximum at $f = f_0 + kt$, then

$$r(t) = f(t) = f_0 + kt \tag{26}$$

Under this condition, we can get the bandwidth from the amplitude of the ridge of PWVD. Further,

we estimate $k_{I,q}$ and $k_{J,q}$ by the ridge of PWVD.

The procedure is shown in Fig.4.

We set $f_q = 8.4$ GHz as an example to see the

PWVD results of the output signals.

It can be divided into four steps.

Step 1: Do PWVD to the output $s_1(n)$ and $s_2(n)$;

Step 2: Extract the ridge of PWVD by equation (25);

Step 3: Detect the amplitude of the ridge of PWVD and calculate the bandwidths corresponding to the amplitude which are denoted as B_{s1} and B_{s2} , respectively;

Step 4: Compute $k_{I,q}$ and $k_{J,q}$ using $B_{s1} = k_{I,q} B_\theta$ and $B_{s2} = k_{J,q} B_\theta$, respectively, and estimate the final Nyquist zone $k_{H,q}$ using equation (9).

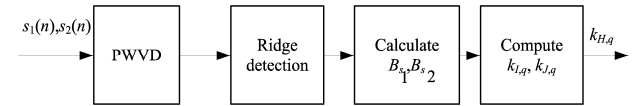


Fig.4. The estimation of Nyquist zone

$k_{I,q}$ $k_{J,q}$ of different components are shown in Table 1.

Table. 1 $k_{I,q}$ $k_{J,q}$ of different components

f_q	$k_{I,q}$	$k_{J,q}$
6. 8GHz	3	1
8.4GHz	4	1
12.6 GHz	1	2
18.2GHz	4	2

After the estimation of $k_{I,q}$ and $k_{J,q}$, we can reconstruct the signal

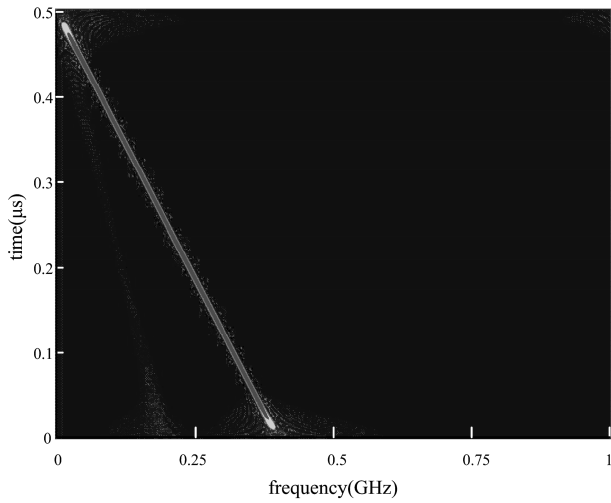
$$d_1(n) = \sum_{q=0}^{Q-1} e^{j[k_{I,q}\theta(nT_s)]} \mu(nT_s - qT_r) \tag{27}$$

$$d_2(n) = \sum_{q=0}^{Q-1} e^{j[k_{J,q}\theta(nT_s)]} \mu(nT_s - qT_r)$$

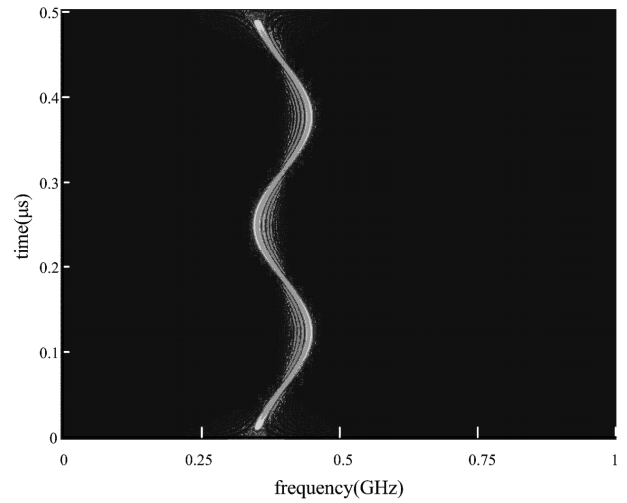
. Multiplying them by $s_1(n)$ and $s_2(n)$ respectively, we get the same equation as follows:

$$z(n) = \sum_{q=0}^{Q-1} e^{j[2\pi(f_q - f_s k_{H,q})nT_s + \phi_q - k_{H,q}\phi_0]} \mu(nT_s - qT_r)$$

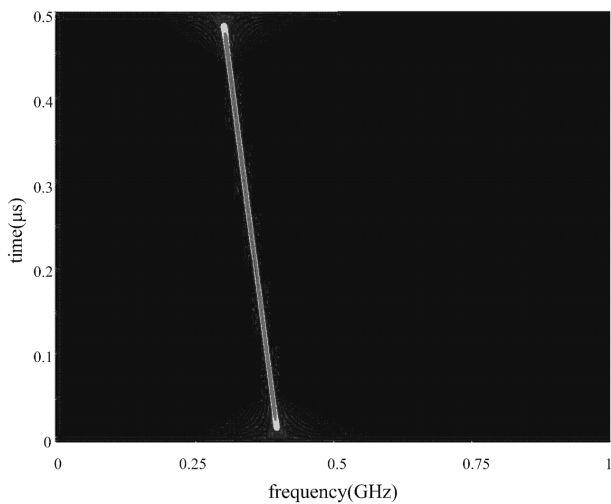
Here, we can see that $z_q(n)$ is independent of the local analogue modulation. Either using SFM or LFM, finally we get the same $z_q(n)$ which is a single-frequency signal whose frequency is $f_q - f_s k_{H,q}$ determined by $f_q, f_s,$ and $k_{H,q}$.



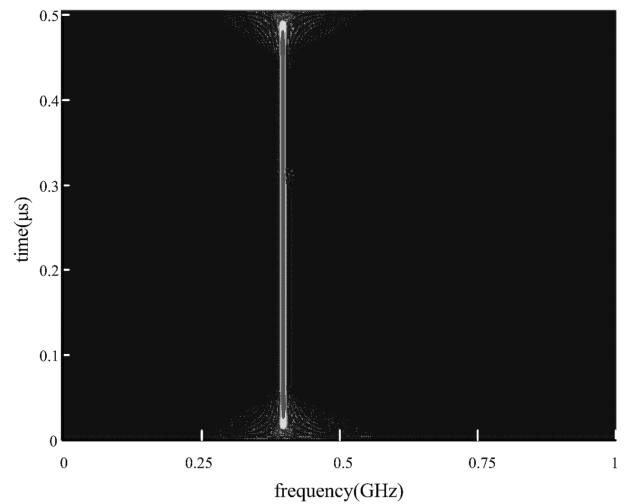
(a) the PWVD of $s_1(n)$ using LFM



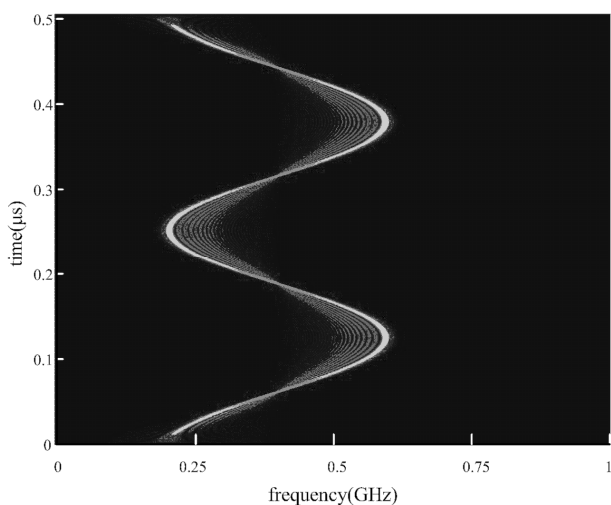
(d) the PWVD of $s_2(n)$ using SFM



(b) the PWVD of $s_2(n)$ using LFM



(e) the PWVD of $z_q(n)$ using LFM /SFM



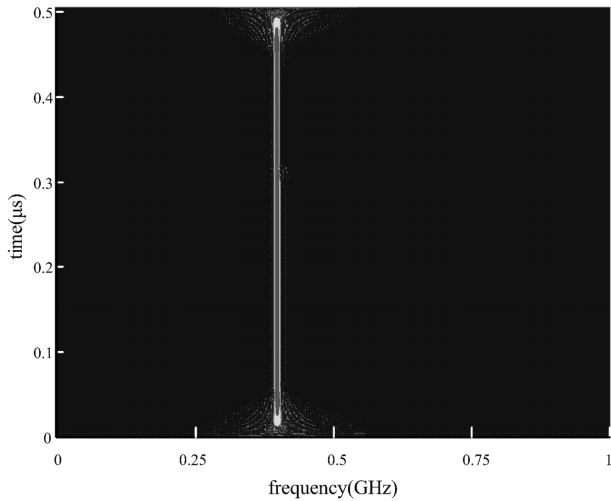
(c) the PWVD of $s_1(n)$ using SFM

Fig.5. The PWVDs for different signals

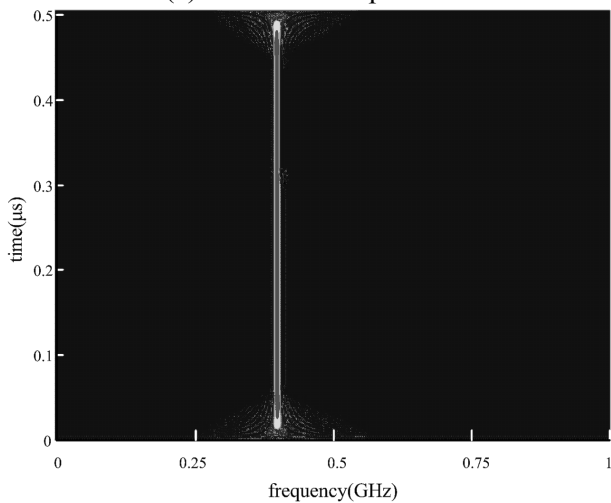
Without loss of generality, we consider the output $z_q(n)$ which is the q th sub-pulse of $z(n)$. Obviously, $z_q(n)$ is a single tone whose carrier frequency is $f_{CNYFR} = f_q - f_s k_{H,q}$. After the estimation of $\hat{k}_{H,q}$, we use a classical algorithm, such as maximum likelihood (ML) to estimate the frequency \hat{f}_{CNYFR} . \hat{f}_q is given by

$$\hat{f}_q = \hat{f}_{CNYFR} + f_s \hat{k}_{H,q} \quad (28)$$

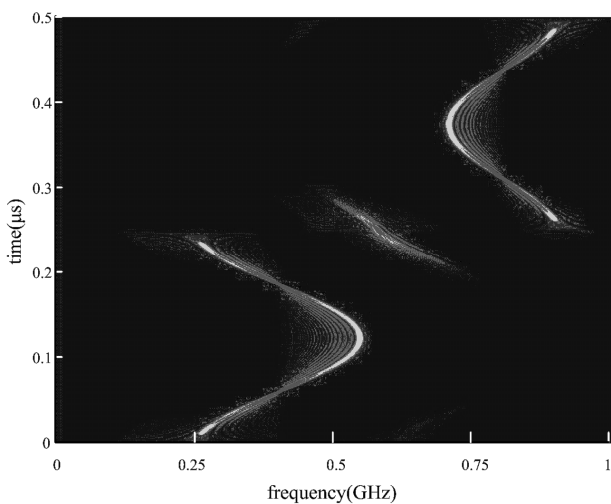
The PWVDs for different signals are shown in Fig.5. For FA signal, the results are shown in Fig.6.



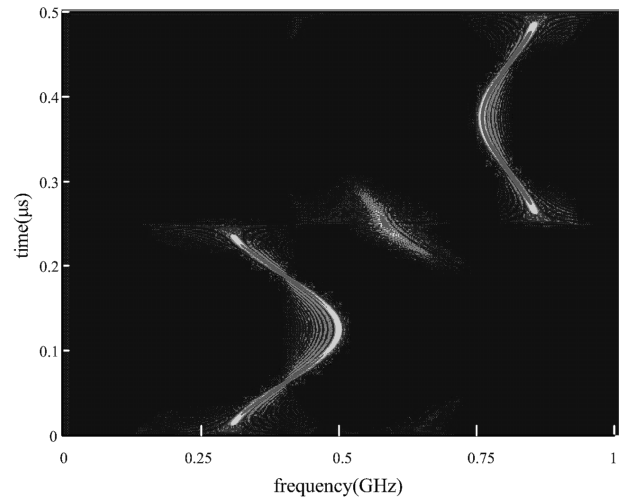
(a) 16.4GHz component



(b) 3.2GHz component



(c) the PWVD of $s_1(n)$ using SFM



(d) the PWVD of $s_2(n)$ using SFM

Fig.6. The PWVDs for FA signal

4. Simulations for the estimation of Nyquist zone

Simulations have been done to verify the performances of the estimation of the Nyquist zone and the hopping frequency. One of the components of the received signal is assumed to be 8.4GHz. The local wideband modulations are SFM and LFM. Their bandwidths are both 100MHz. The number of channels could be one or two. The pulse width is $0.5\mu s$. The SNRs are from $-5dB$ to $10dB$ where the noise is Gaussian and white. Each signal was run 200 times of Monte-Carlo experiment. The performance is evaluated by the probability of correct decision (PCD) and normalized root mean squared error (NRMSE) of the estimated frequency:

$$PCD = \frac{R_T}{S_T} \tag{29}$$

$$NRMSE = \frac{\sqrt{\frac{1}{S_T} \sum_{k=1}^{S_T} (\zeta_k - \zeta)^2}}{\zeta} \tag{30}$$

where

- R_T time of correct decision;
- S_T time of experiment, $S_T = 200$;
- ζ the parameter to be estimated;
- ζ_k the value of estimation.

In each experiment, if the estimation of Nyquist zone is right, R_T add 1. The results are shown in Fig.7 and Fig.8. The CNYFR with analogue modulation of LFM has the best performance and accuracy of hopping frequency estimation is acceptable when the SNR is above $0dB$, because the

PCD of Nyquist zone is above 90% when the SNR is greater than -1dB.

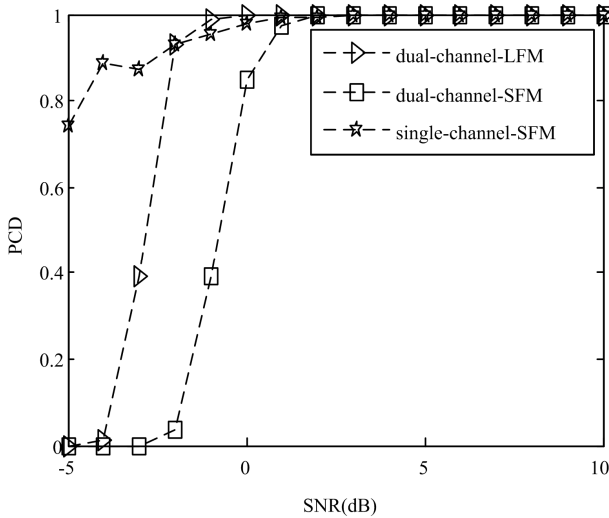


Fig.7. The PCD of the estimated Nyquist zone

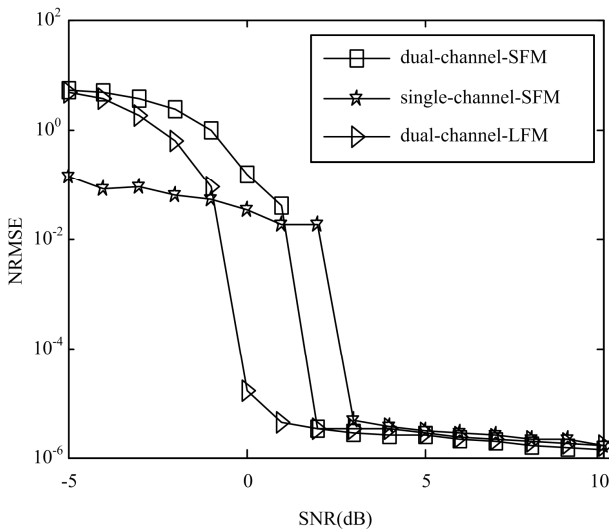


Fig.8. NRMSE of estimated hopping frequency

Firstly, it is more accurate for linear modulation to find the maximum and minimum of the ridge than sinusoidal modulation. Moreover, the amplitudes, $k_{l,q}$ and $k_{j,q}$, are easier to be estimated. Secondly, dual-channel reduces the difficulty of the realization of analog modulation and widens the interception bandwidth which is important for the intercept of other wideband signals such as LFM, et al. To sum up, the CNYFR with analog modulation of LFM can achieve the best performance.

Letting the SNR=3dB, we make one time simulation to estimate $k_{l,q}$, $k_{j,q}$, and f_q . The results are shown in Table 2, Table 3 and Table 4. It is shown that all the results are in accord with the statistics ones.

Table. 2 Using SFM-Dual

f_q	\hat{f}_q	$\hat{k}_{l,q}$	R or W	$\hat{k}_{j,q}$	R or W
6.8GHz	6.800028GHZ	3	R	1	R
8.4GHz	8.3999897GHZ	4	R	1	R
12.6 GHz	12.600007GHZ	1	R	2	R

Table. 3 Using LFM-Dual

f_q	\hat{f}_q	$\hat{k}_{l,q}$	R or W	$\hat{k}_{j,q}$	R or W
6.8GHz	6.799954GHZ	3	R	1	R
8.4GHz	8.400009GHZ	4	R	1	R
12.6 GHz	12.600007GHZ	1	R	2	R

Table. 4 Using SFM-single

f_q	\hat{f}_q	$\hat{k}_{H,q}$	R or W
6.8GHz	6.799992GHZ	3	R
8.4GHz	8.399989GHZ	4	R
12.6 GHz	12.599987GHZ	6	R

Notes: R stands for 'right', W 'wrong'.

5 Conclusions

Based on the structure of the CNYFR, the interception of the FA radar signal can be achieved. Then, we adopt PWVD to estimate Nyquist zone. The CNYFR can estimate the hopping frequencies of the received signal as a result of the reconstruction signal generated by the information of the zone and improve the reliability of the structure NYFR using the analogue modulation of LFM. The method of DDS +DAC in the CNYFR overcomes the sensitivity of noise in the NYFR to generate the wideband modulation. This digital method is easy to be controlled and the implement needs to do the further research.

Simulation results show that in the case of the CNYFR with analogue modulation of LFM, the PCD of the Nyquist zone is above 90% when the SNR is greater than -1dB, and NRMSE of the hopping frequency can be less than 10^{-4} when the SNR is greater than 0dB. The performance of the CNYFR with analogue modulation of LFM is better than the one of SFM.

References:

[1] J. R. Bellegarda, S. V. Maric, E. L. Titlebaum, The hit array: a synthesis tool for multiple access frequency hop signals, *IEEE*

- Transactions on Aerospace and Electronic Systems*, Vol.29, No.3, 1993, pp.624-635.
- [2] K. Morrison, Effective bandwidth SF-CW SAR increase using frequency agility, *IEEE Aerospace and Electronic Systems Magazine*, , Vol.21, No.6, 2006, pp.28-32.
- [3] K. Becker, Passive localization of frequency-agile radars from angle and frequency measurements, *IEEE Transactions on Aerospace and Electronic Systems*, Vol.35, No.4, 1999, pp.1129-1144.
- [4] S. R. Rogers, On analytical evaluation of glint error reduction for frequency-hopping radars, *IEEE Transactions on Aerospace and Electronic Systems*, Vol.27, No.6, 1991, pp. 891-894.
- [5] G. Lellouch, P. Tran, R. Pribic, P. van Genderen, OFDM waveforms for frequency agility and opportunities for doppler processing in radar, *IEEE Radar Conference*, 2008.
- [6] E. J. Candes, T. Tao, Near-optimal signal recovery from random projections: universal encoding strategies? *IEEE Transactions on Information Theory*, Vol.52, No.12, 2006, pp. 5406-5425.
- [7] D. L. Donoho, Compressed sensing, *IEEE Transactions on Information Theory*, Vol.52, No.4, 2006, pp. 1289-1306.
- [8] M. A. Herman, T. Strohmer, High-resolution radar via compressed sensing, *IEEE Transactions on Signal Processing*, Vol.57, No.6, 2009, pp. 2275-2284.
- [9] J. Ma, Compressed sensing for surface characterization and metrology. *IEEE Transactions on Instrumentation and Measurement*, Vol.59, No.6, 2010, pp. 1600-1615.
- [10] L. C. Potter, E. Ertin, J. T. Parker, M. Cetin, Sparsity and compressed sensing in radar imaging. *IEEE Proceedings*, Vol.98, No.6, 2010, pp. 1006-1020.
- [11] J. Provost, F. Lesage, The application of compressed sensing for photo-acoustic tomography. *IEEE Transactions on Medical Imaging*, Vol.28, No.4, 2009, pp. 585-594.
- [12] P. Flandrin, P. Borgnat, Time-frequency energy distributions meet compressed sensing, *IEEE Transactions on Signal Processing*, Vol.58, No.6, 2010, pp. 2974-2982.
- [13] J. A. Tropp, J. N. Laska, M. F. Duarte, J. K. Romberg, R. G. Baraniuk, Beyond Nyquist: efficient sampling of sparse bandlimited signals, *IEEE Transactions on information theory*, Vol. 56, No. 1, 2010, pp. 520-544.
- [14] J. N. Laska, S. Kirolos, M. F. Duarte, T. S. Ragheb, R. G. Baraniuk, Y. Massoud, Theory and implementation of an analog-to-information converter using random demodulation, *IEEE International Symposium on Circuits and Systems*, 2007, pp. 1959 – 1962.
- [15] J. Romberg. Compressive sensing by random convolution. *2nd IEEE International Workshop on Computational Advances in Multi-Sensor Adaptive Processing*, 2007, pp. 137 – 140.
- [16] J. A. Tropp, M. B. Wakin, M. F. Duarte, D. Baron, R. G. Baraniuk, Random filters for compressive sampling and reconstruction, *IEEE International Conference on Acoustics, Speech and Signal Processing*, 2006, pp. III.
- [17] D. Takhar, J. N. Laska, M. Wakin, M. F. Duarte, D. Baron, S. Sarvotham, K. F. Kelly, R. G. Baraniuk, A new compressive imaging camera architecture using optical-domain compression, *Computational Imaging*, 2006.
- [18] G. L. Fudge, R. E. Bland, M. A. Chivers, S. Ravindran, J. Haupt, P. E. Pace, A Nyquist folding analog-to-information receiver, *42nd Asilomar Conference on Signals, Systems and Computers*, 2008, pp. 541-545.